HEAT ENGINEERING

NONLINEAR HEATING SYSTEM OF MODULAR-POURING AND PLATFORM FURNACES FOR FIRING BULK MATERIALS

A. I. Nizhegorodov[1,2]

This article presents a design of a suspended nonlinear heating system of modular-pouring and platform furnaces for firing vermiculite and other bulk materials. The previous design of linear heating systems did not provide uniform heating of heat-treated materials, and the material in the near-wall zones did not receive sufficient thermal energy. In addition, the overheating of the central zone increased the burnout frequency of the heaters themselves, which affected the furnace reliability. Accordingly, the use of a nonlinear heating system reversed this distribution. The power of the near-wall heater exceededA that of the central one by 1.2 – 1.36 times, depending on the ratio of the diameters of thin and thick (4 mm in diameter) heaters. Moreover, not only their electric power but also the fluxes of thermal radiation falling on the surface of the hearth increased, which resulted in an increase in the temperature of the material being processed. The obtained values of the temperature of vermiculite grains in the near-wall zones of the firing module exceeded the temperature of vermiculite in the central zone by 26%, which is sufficient for the high-quality swelling of the material. With the use of a nonlinear heating system, a redistribution of temperatures on the heated surfaces occurred toward relatively cold near-wall zones, such that the thermal presentation changed to the opposite and the cold near-wall zones became relatively hot.

Keywords: nonlinear heating system, modular-pouring furnace, platform furnace, vermiculite, non-uniform temperature distribution, relative electrical power, relative temperature.

INTRODUCTION

In 2015, the first experimental electric platform furnace with a swing hearth was built and tested, which paved the way for a new concept of furnace units for firing vermiculite and other thermally activated bulk materials [1]. This concept also revealed the possibility of bringing a specific energy consumption of its firing up to 65 – 80 mJ/m³ depending on the type and dimension of the feedstock.

Due to their design aspects (e.g., the use of inclined modules with accelerating movements of fired materials), the previous concept of modular-pouring furnaces did not achieve such indicators until new original designs were developed, which enabled almost doubling the productivity with a constant power consumption [2, 3]. The new nonlinear heating system, suitable for use in both types of furnace

units, is expected to ensure the quality of firing and an additional increase in their energy efficiency.

The main characteristics of platform furnaces include the minimized working space of firing modules, new design of quick-detachable suspended heating systems, and transportation of fired raw materials in a thermal field at a constant speed with a continuous flow of particles of vermiculite concentrate or other materials. Accordingly, not only high energy efficiency but also maximum reliability is achieved.

However, furnaces with a new design also incur one of the disadvantages of electric modular-pouring furnaces, that is, an uneven thermal field in the firing space, which requires a certain overestimation of the thermal power to ensure a high-quality heat treatment of raw materials.

The first furnaces had a heating system in the form of a set of single heaters made of nichrome strips, connected in a serial electrical circuit and located on the base of the firing

[1] Irkutsk National Research Technical University, Irkutsk, Russia.
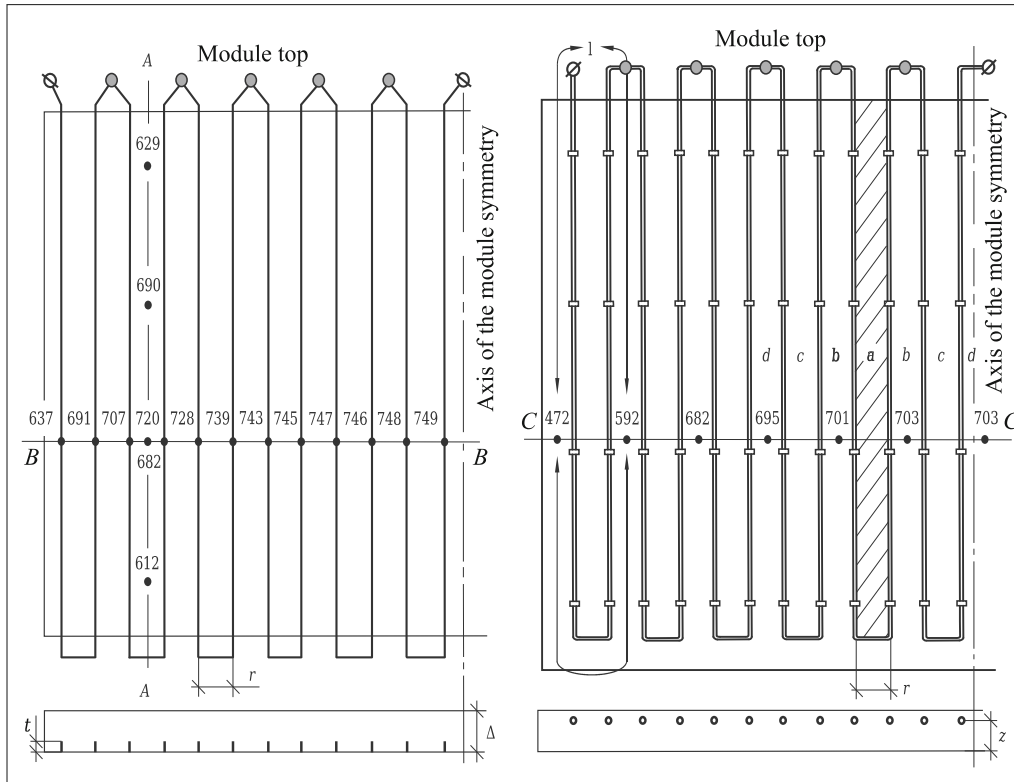[2] nastromo_irkutsk@mail.ru

Fig. 1. Linear heating systems of modular-pouring (*a*) and platform furnaces (*b*)

modules. This scheme had to be rejected when using suspended heating systems [1 – 3].

Accordingly, the present work aims to improve modular-pouring and movable hearth furnaces using a new design of quick-detachable suspended nonlinear heating systems in firing modules.

ANALYSIS OF HEATING SYSTEMS OF ELECTRIC MODULAR-POURING FURNACES

Figure 1 shows the heating systems of the firing modules of two furnace types, namely, an electric module-pouring furnace made of nichrome strips (Fig. 1*a*) and a platform furnace made of nichrome wires (Fig. 1*b*). System 1 is installed in a furnace at an angle of 45° to the horizon, like the module itself, coupled with the other two systems for pouring the heat-treated material under the influence of the particle gravity, presenting the operation of gravity chutes [4]. System 2 can be installed horizontally and obliquely sloping, above the oscillating hearth of the platform furnace, depending on its design. Both of them belong to linear heating systems, in which the spacing of the electric heaters and their cross-section are constant.

The modular-pouring a furnace used for the temperature measurements (Fig. 1*a*) included three firing modules, each having 12 heaters. Section *A–A* selectively shows the temperatures on the firing surface between the heaters, and sec-

tion *B–B* shows the temperatures of the heaters themselves. The change in temperature along the longitudinal section *A–A* is associated with the inclined position of the modules, which causes a thermal air draft in the firing space and cooling of their refractory base in the lower and upper parts. This disadvantage is completely eliminated in platform furnaces with a movable hearth. A platform with a hearth in such a furnace performs low-frequency asymmetric vibrations, which result in a vibratory transport effect being studied well and widely used in technology [5].

Figure 2*a* shows a dependence graph of the temperature along section *A–A* (Fig. 1) on the measurement point along the entire length of the refractory surface of the firing module, plotted according to the experimental data.

With an inclined position of the firing modules, the temperature of their surfaces, along with the swelling grains of vermiculite or other heat-treated material rolls, insignificantly changed, reaching the highest value approximately in the center of the module. Such a pattern is present not only in section *A–A* but also in any of the longitudinal sections. In this case, in the near-wall zones of the modules, the absolute values of temperatures are somewhat lower than those in section *A–A*. To eliminate the longitudinal temperature gradient, the heat-treated material movement at a constant rate should be ensured at the horizontal position of the firing surface, which completely excludes the air draft [4], leading to inhomogeneity.
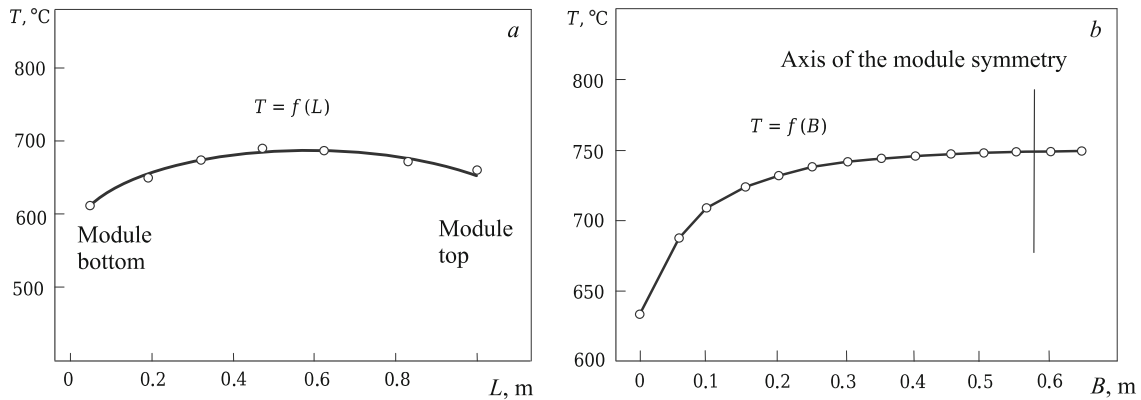
Fig. 2. Change in the surface temperature of the module along longitudinal section *A–A* (*a*) and the temperature distribution of the heaters made of nichrome strips along section *B–B* (*b*)

Another drawback is the uneven temperature distribution of heaters themselves over the width of the modules. Figure 2*b* shows a dependence graph of the heater temperatures along section *B–B* (Fig. 1*a*) from the near-wall zone of the module on the left to the axis of its symmetry, plotted according to the experimental data [4]. The temperatures are distributed not only on electric heaters but also on the surface of modules in the furnaces of both types. Figure 1b presents the experimentally obtained temperature distribution on the surface of the movable hearth platform of a horizontal platform furnace, and Fig. 3 presents a graph of this distribution across the module width.

The heat-treated material in the firing process in the lateral zones of the modules does not receive the necessary thermal energy, and this limitation requires an increase in the thermal and electrical power of the furnace unit and is accompanied by their unjustified losses. A furnace operating in this mode consumes more electricity than that required in the absence of a temperature gradient.

DEVICE AND OPERATION
OF THE ELECTRIC FURNACE
WITH A SUSPENDED HEATING SYSTEM

A platform electric furnace with a movable hearth and suspended heating system for firing vermiculite concentrates is presented in Fig. 4. The raw material is fed by the dispenser onto the hearth surface *1* made of heat-resistant steel, connected to the platform *2*, and mounted on rollers *3* in the guide rails *4* of the frame. When the adjustable electric motor *5* is started, its eccentric shaft *6* through the plunger *7* compresses and releases the spring *8*, which introduces the platform with the hearth into the mode of near-resonance oscillations *x* at a frequency approximately equal to the natural frequency of the platform of 8 – 9 Hz.

In such a dynamic system, a special nonlinear elastic element *9* plays a key role [6] by exerting asymmetric oscillations, in which the heat-treated material particles move in
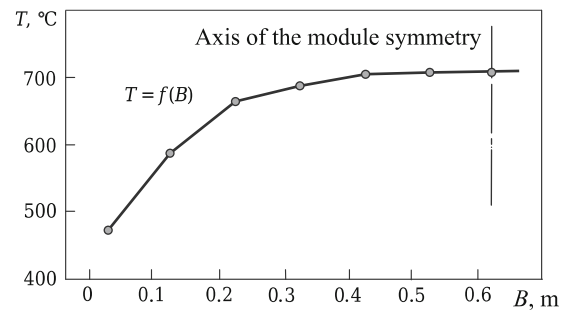

Fig. 3. Experimental temperature distribution on the surface of the movable hearth of the platform furnace.

pulsating unidirectional movements with a constant average speed determined by the frequency and amplitude of platform oscillations [5].

The flow of the material particles moves in a non-uniform thermal field created by electric heaters *10* fixed by clamps *11* and fasteners *12* in the form of shackles *13* under the thermal cover of the furnace *14*.

The process of vermiculite firing is fast and lasts from 2.5 to 3.2 sec depending on the size group of the concentrate [1].

The linear heating system of the considered furnace consists of wire heaters with an equal diameter and cross-sectional area. Hence, the second disadvantage noted above persists because these heaters do not provide equal heating temperatures for expanded vermiculite or other heat-treated materials throughout the width of the module. In the central part, the bulk material on any selected fragment of the stock pan receives significantly more thermal energy from the heaters located above it and from neighboring heaters to the right and left of it. The material on the fragment highlighted in the near-wall zones will receive less heat, only from the heaters located above it and from the neighboring heaters located only on one side.
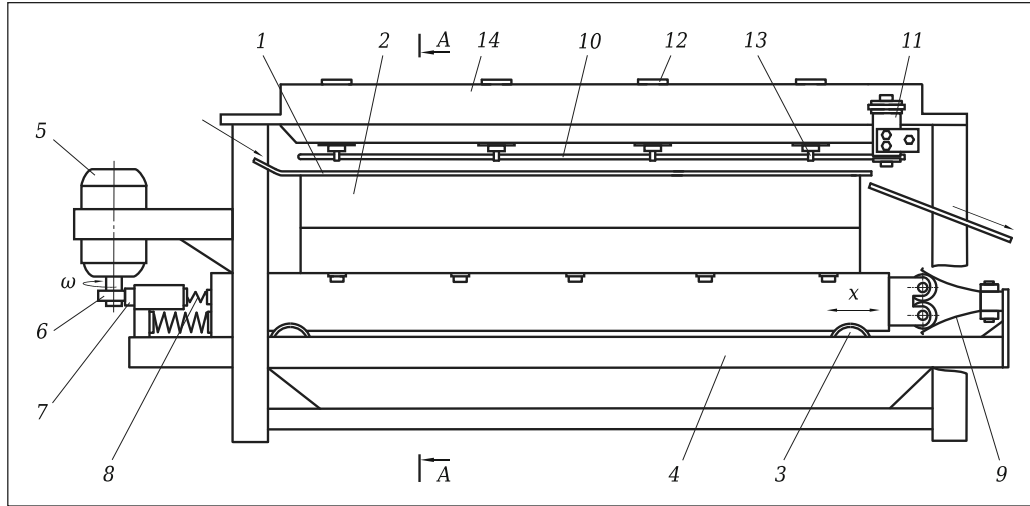
Fig. 4. Device of a single-module single-phase electric furnace with a suspended heating system.

If we take into account that the heaters fixed along the thermal lid edges above the near-wall zones of the stock pan of the movable heartha are less heated than the heaters in the central zone, then it is clear that the bulk material moving in these zones also receives less heat energy. Therefore, bulk materials (e.g., vermiculite) in the central zone of the module swell qualitatively and have the lowest bulk density, and the vermiculite leaving the furnace remains under-expanded at its edges and has a relatively high density. This difference in bulk densities was checked during the operation of an experimental platform furnace. The findings prove that, in general, the vermiculite concentrate swells poorly, i.e., not to the full extent, as it could swell if the temperature of the heaters located at the edges of the stock pan was higher than the temperature of the heaters in its center, and the temperature of all the stock pan zones would be equal.

Due to overheating, the burnout of the heating elements in the module central zone occurs much more often than in the near-wall zones, which reduces the furnace unit reliabil-

ity. This condition is another disadvantage of linear suspension systems and requires a redistribution of thermal power.

The influence of neighboring electric heaters on the heating zone under the selected pair of heaters of the refractory surface (shaded zone a in Fig. 1b) was studied analytically and verified experimentally on one of the pilot-industrial furnaces [4].

Figure 5 shows the distribution of the angular coefficients φ presenting the proportion of heat power flows passing from neighboring pairs of heaters [7] from zones b, c, and d (Fig. 1b) in the total amount of heat power falling on the surface of the selected zone a. Already in zone c, the angular coefficient is 0.045, and the angular coefficients ratio 0.24/0.045 is 5.3. In the third of the selected zones d, the slope φ_d is 10 times less than in the main zone a with the coefficient φ_a of 0.24. Therefore, the influence of the neighboring zone 3 can be ignored in general.

The linear system must be restructured by determining the cross-sections of the electric heaters, depending on their location in the furnace module.

NONLINEAR SUSPENDED HEATING SYSTEM

To ensure the most uniform temperature distribution on the surface of the module of a platform or modular-pouring furnace, a nonlinear heating system has been developed and patented [8].

Figure 6 shows the simplest suspended nonlinear heating system (section A–A in Fig. 4) with a stepped transition of heaters from one diameter to another. It comprises heaters of small-diameter D_a 1, 2, located in the near-wall zone, and heaters 3 with a large diameter D_b. In this case, fasteners 4 and 5 have different lengths, such that the gap z relative to the surface of the stock pan 6 is equal (Fig. 6). All heaters were held using their fasteners under a thermal lid 7 made of a ceramic-vermiculite plate edged with an angle 8 and fixed
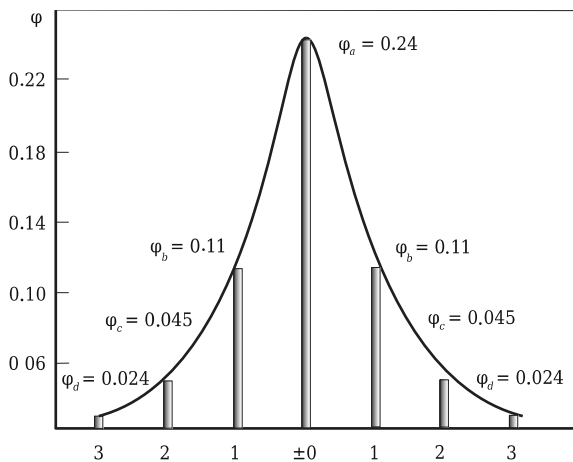

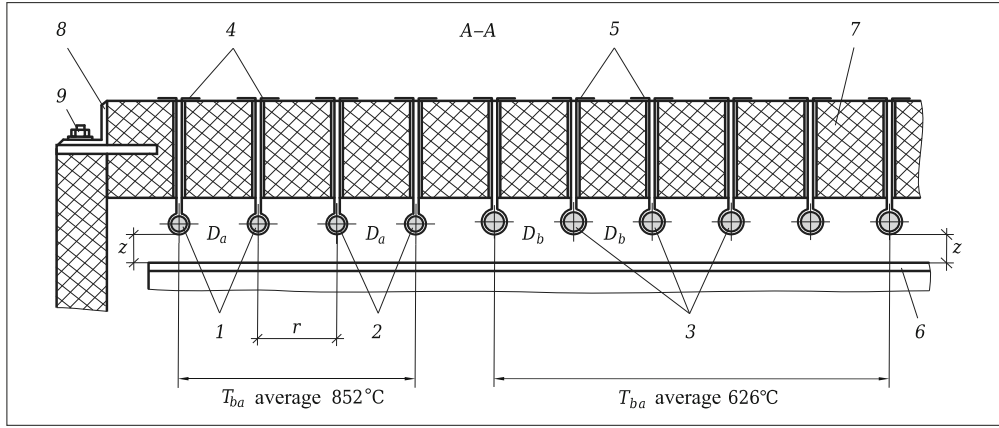**Fig. 5.** Distribution of angular coefficients.

Fig. 6. Suspended nonlinear heating system (section of the thermal cover *A–A* according to Fig. 4).

with a threaded connection *9* on the thermal insulating side wall of the firing module.

REDISTRIBUTION OF THERMAL POWER AND TEMPERATURE OF THE HEATING SYSTEM

The electric power balance equation for the nonlinear heating system presented in Fig. 6 can be written as follows

$$IU = 2nIU_1 + mIU_2, \qquad (1)$$

where I is the current in the heater circuit, A; U is the phase voltage at the edges of the heating system, V; U_1 is the voltage at the ends of wire heaters with diameter D_a, V; U_2 is voltage at the ends of wire heaters with diameter D_b, V; n is the number of heaters with a diameter D_a at one of the near-wall (edge) zones; and m is the total number of heaters with a diameter D_b.

Let us present voltages U_1 and U_2 through the specific resistivity of nichrome ρ, lengths l_a and l_b, and diameters of wire heaters as follows:

$$U_1 = I\rho \frac{4l_a}{\pi D_a^2}, \qquad (2)$$

$$U_1 = I\rho \frac{4l_b}{\pi D_b^2}, \qquad (3)$$

Substituting the equations obtained into Eq. (1) and transforming it, taking into account the equality of the lengths of all heaters $l_a = l_b = 1$, we obtain the following:

$$U = \frac{4I\rho l}{\pi} \left(\frac{2n}{D_a^2} + \frac{m}{D_b^2} \right), \qquad (4)$$

Let us solve Eq. (4) with respect to the current in circuit *A*:

$$I = \frac{U\pi}{4\rho l \left(\dfrac{2n}{D_a^2} + \dfrac{m}{D_b^2} \right)}. \qquad (5)$$

For $n = 2$ and $m = 8$, setting the value of D_b equal to 4 mm (const) and a number of D_a values, one can plot the dependence of the current I in the heater circuit on the diameter D_a of small-diameter near-wall heaters (Fig. 7). The calculation according to Eq. (5) was performed with D_b of 0.004 mm, l of 0.8 m, and nichrome density ρ of 1.1×10^{-6} Ω·m [9].

By setting the values of diameter D_a, for example, 2.8, 3.0, 3.2, and 3.5 mm with the corresponding values of I of 194, 204, 220, and 237 A, we obtain a loss in voltage and electric power on one heater and on four heaters as follows:
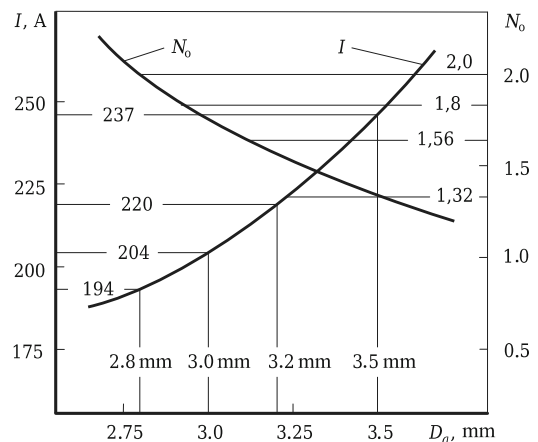

Fig. 7. Change in current I and relative power N_o of single heaters with diameter D_a.

– With D_a of 2.8 mm, $U_1 = 27.7$ V and $N_1 = 5.4$ kW on one heater and 110.8 V and 21.4 kW on four heaters, respectively.

– With D_a of 3.0 mm, $U_1 = 25.5$ V and $N_1 = 5.2$ kW on one heater and 102.0 V and 20.9 kW on four heaters, respectively.

– With D_a of 3.2 mm, $U_1 = 24.1$ V and $N_1 = 5.3$ kW on one heater and 96.4 V and 21.2 kW on four heaters, respectively.

– With D_a of 3.5 mm, $U_1 = 21.7$ V and $N_1 = 5.2$ kW on one heater and 86.8 V and 20.8 kW on four heaters, respectively.

For different values of the current I, the voltage drop across heaters with a diameter D_b of 0.004 mm will also change the voltage drop, and the electric power on one and eight heaters will be as follows:

– With $I = 194$ A, $U_2 = 13.59$ V and $N_2 = 2.64$ kW on one heater and 108.7 V and 21.1 kW on eight heaters, respectively.

– With $I = 204$ A, $U_2 = 14.35$ V and $N_2 = 2.94$ kW on one heater and 114.8 V and 23.5 kW on eight heaters, respectively.

– With $I = 220$ A, $U_2 = 15.44$ V and $N_2 = 3.41$ kW on one heater and 123.5 V and 27.2 kW on eight heaters, respectively.

– With $I = 237$ A, $U_2 = 16.60$ V and $N_2 = 3.95$ kW on one heater and 133.0 V and 31.6 kW on eight heaters, respectively.

When checking the sums of the voltage drop in the entire heating system ($U_1 + U_2$), the values of $217.2 – 219.9$ V (≈ 220 V) were obtained.

When the powers N_1 and N_2 are summed up, an increase in the total electrical power received by the heating system of the furnace is noted (42.7, 45.1, 48.5, and 52.2 kW).

Let us take the equal relative powers at single heaters:

$$N_o = N_1 / N_2, \qquad (6)$$

– With D_a of 2.8 mm $N_o = N_1/N_2 = 5.4/2.64 = 2.0$.
– With D_a of 3.0 mm $N_o = N_1/N_2 = 5.2/2.94 = 1.8$.
– With D_a of 3.2 mm $N_o = N_1/N_2 = 5.3/3.41 = 1.56$.
– With D_a of 3.2 mm $N_o = N_1/N_2 = 5.2/3.95 = 1.32$.

Evidently, the electrical power of near-wall heaters with a diameter D_a increases with its decrease relative to the power on each of the eight central heaters with a diameter D_b (Fig. 7). Consequently, the fluxes of thermal power emitted by the heaters in the near-wall zones, falling on the surface of the furnace heartha, will now be greater than those in the central part of the module, as was the case in the prototype presented in Fig. 4 [1].

Let us determine the heating temperatures of the heaters through their electrical power using Eq. [9]:

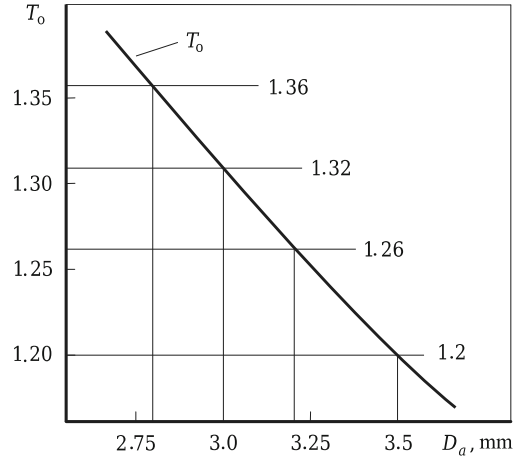$$\frac{IU}{f} = \sigma T^4, \qquad (7)$$

Fig. 8. Dependence of T_o on the small heater diameter D_a.

where IU is the electrical power of one small-diameter heater N_1 or a large heater N_2; f is the total surface area of a heat-emitting heater of length l, m^2; σ is the Stefan – Boltzmann constant, equal to 5.67×10^{-8} W/(m^2·K^4) [10]; and T is the temperature on the surface of the corresponding heaters, K.

For further analysis and calculations, the following assumptions were made:

– The phase voltage is maintained constant and equal to 220 V; cables and electrical devices are not part of the furnace, and losses in them are not taken into account.

– The active resistance of nichrome [9] is three orders of magnitude greater than that of the inductive one, and it can be neglected in the same way as the influence of the electromagnetic field of the heaters on the formation of the inductive resistance of neighboring heaters.

– In the operating temperature range of the furnace (750 – 850°C), the share of the radiant energy of the heaters in the visible part of the spectrum (with wavelength $\lambda = 0.4 – 0.76$ μm) is no more than 0.04% [10]. Therefore, the losses radiant energy was also not taken into account.

– The load on the network from a working furnace is active, so almost all electrical power with an error of no more than $1 – 1.5\%$ was converted into thermal radiation.

– The skin effect, leading to the flow of current mainly in the surface layer of the conductor and a slight increase in active resistance, does not violate the approximate balance shown in Eq. (7).

From Eq. (7), we express the temperature of the heaters T_a and T_b, K:

$$T_a = \sqrt[4]{\frac{IU_1}{\sigma f_a}}, \qquad (8)$$

$$T_b = \sqrt[4]{\frac{IU_2}{\sigma f_b}}. \qquad (9).$$

Using Eq. (8), we calculate the average temperature T_a from four power values on one small heater N_1 (5.4, 5.2, 5.3, and 5.2 kW), i.e., $T_a = 1195°C$.

Then, using Eq. (9), we determine the temperatures T_b on a large heater at different values of D_a at the corresponding powers N_2 and relative temperatures T_a/T_b:

– At $N_2 = 2.64$ kW, $T_b = 914°C$, $T_o = 1244/914 = 1.36$.
– At $N_2 = 2.94$ kW, $T_b = 942°C$, $T_o = 1244/942 = 1.32$.
– At $N_2 = 3.41$ kW, $T_b = 987°C$, $T_o = 1244/987 = 1.26$.
– At $N_2 = 3.95$ kW, $T_b = 1036°C$, $T_o = 1244/1036 = 1.2$.

The value of T_o changes with a decrease in the small diameter to a lesser extent than the relative electrical power N_o (Fig. 7), from 1.2 to 1.36 (Fig. 8). A decrease in the diameters D_a of the near-wall heaters relative to the heaters of the central zone of the firing module with a diameter D_b leads to a significant redistribution of temperatures on the heating surfaces in favor of relatively cold near-wall zones. Thus, the disadvantage of the prototype (Fig. 4) with a suspension system of identical heating elements is eliminated.

Let us consider the temperature distribution on the continuous surface of expanded vermiculite, distributed without gaps between the particles along the surface of the furnace heartha. Using the method of calculating a suspended heating system [11], we determine the temperature under small (D_a) and large (D_b) heaters:

$$T_v = \sqrt[4]{\frac{1}{\sigma f_a}\left[Q_{ef} - Q_{rf}\left(\frac{1-\varepsilon_v}{\varepsilon_v}\right)\right]}, \qquad (10)$$

where T_v is the temperature of the vermiculite under the heater (in one working chamber [11]); f_a is the surface area of a part of the hearth under one heater; Q_{ef} and Q_{rf} are the effective and resultant heat power fluxes on the surface of the hearth part under the heater, respectively, determined by Eq. [11]:

$$Q_{ef} = 6\varepsilon_n IU(1 + \rho_n\varphi_{12})(\varphi_{13} + \varphi_{34}\varphi_{14}\rho_n)/(1 - \rho_e^2\varphi_{34}^2), \quad (11)$$

$$Q_{rf} = \varepsilon_n\sigma T_h^4 f(1 + \rho_n\varphi_{12})(\varphi_{12} - 1)\varphi_{12} + Q_{rf}\varphi_{31} + Q_{ef}\varphi41, \quad (12)$$

where ε_n is the degree of blackness of nichrome, $\varepsilon_n \approx 0.96$ [9]; ρ_n is reflective surface of nichrome, $\rho_n \approx 0.04$ [9]; ρ_e is reflectivity of expanded vermiculite, $\rho_e \approx 0.232$ [12]; T_h is the heater temperature; and φ_{12}, φ_{13}, φ_{31}, φ_{34}, φ_{14}, and φ_{41} are the average angular coefficients determined by the stretched filament method and reflecting a part of the effective radiation of some surfaces falling on others [13].

The average temperatures of vermiculite under small and large heaters are obtained using Eqs. (10), (11), and (12) according to the method in [11] with the initial data of $D_b = 4$ mm, $l = 0.8$ m, $z = 35$ mm, and $r = 42$ mm, with a height of the firing space (between the hearth and thermal lid) of 44 mm, with four small heaters and eight large heat-

ers, the previously obtained values of the voltages U_1 and U_2 and the current I of 194 A (with a small-diameter D_a of 2.8 mm), under small heaters with a diameter D_a of 2.8 mm, T_{va} of 852°C, under the large heaters with a diameter D_b of 4.0 mm T_{vb} of 626°C.

The resulting values of the vermiculite temperature are sufficient for its full expansion [11] and are distributed as required (Fig. 6). For instance, in the central part of the firing module, the average temperatures are lower ($\approx 626°C$) than in the near-wall zones ($\approx 852°C$) by approximately 26%.

In the prototype (Fig. 1b), the average temperatures in the zones of the near-wall $T_{nw} = (472 + 592)/2 = 532$ and central $T_c = (682 + 695 + 701 + 703)/2 = 695$ and their ratio $T_{nw}/T_c = 532/695 = 0.765$ indicate that the heating of vermiculite in the prototype is 23.5% lower in the near-wall zone. This case is what should have been changed. When a nonlinear heating system is used, the picture changes to the opposite, and cold near-wall zones become relatively hot.

This result is attributed to the average temperatures because they were calculated without considering the influence of neighboring heaters (Fig. 5). However, this influence does not exceed 10 – 12% [14] and therefore does not significantly change their distribution.

The obtained temperature distribution in vermiculite grains lying on the furnace heartha is a zonal temperature model because the heat energy cannot be distributed discretely. In fact, a smoothed picture is obtained.

Because the electrical system of the kiln unit is controllable, when firing other bulk materials or vermiculite of other size groups, a change in the electrical power and temperature regime is required.

The main disadvantage of electric modular-pouring and platform furnaces with suspended heating systems, i.e., uneven thermal field in the firing space, has been eliminated, which will allow avoiding an overestimation of power consumption to ensure a high-quality heat treatment of raw materials.

CONCLUSIONS

The design of quick-detachable suspended heating systems for modular-pouring and platform furnaces for firing various bulk materials has been improved.

In furnaces with linear heating systems, assembled from wire heaters with equal diameters, the material in the process of firing in the near-wall zones of the modules did not receive sufficient thermal energy, which required an increase in the electric power of the furnace and was accompanied by significant losses. The furnace in this mode consumed more electricity than that required in the absence of temperature distribution over the width of the module. At the same time, in the central zone, the material to be fired received more heat from its heaters, and the material in the near-wall zones received less heat. The vermiculite in the central zone of the module qualitatively expanded with the lowest density, and

the vermiculite that came out of the furnace from the near-wall zones remained under-expanded and had a relatively high density. In addition, the overheating of the central zone increased the frequency of burnout of the heaters, which affected the furnace reliability.

The use of a suspended heating system, in which heaters with a smaller diameter are placed in the near-wall zones of the firing module than in the central zone, changed this distribution to the opposite. The electric power of one near-wall heater exceeded the power of the central one by 1.2 – 1.36 times, depending on the ratio of the diameters of thin (2.8 – 3.5 mm in diameter) and thick (4 mm in diameter) heaters. Clearly, this condition increased not only the electrical power of the near-wall heaters but also the heat fluxes emitted by them, falling on the surface of the furnace hearth. This condition also led to an increase in the temperature of the material being processed (in the considered case, vermiculite). The obtained values of the temperature of vermiculite grains in the near-wall zones of the firing module exceeded the temperatures of vermiculite in the central zone by 26%, and they are sufficient for the high-quality swelling of the material.

With a nonlinear heating system, a redistribution of temperatures on the heated surfaces took place in favor of the previously relatively cold near-wall zones, and the thermal pattern changed to the opposite, such that the cold near-wall zones became relatively hot.

REFERENCES

1. A. I. Nizhegorodov, "Testing of a new alternative electric furnace for firing vermiculite concentrates," *Izvest. Tomsk. Politekhnich. Univ. Inzhinir. Georesurs.*, **329**(4), 142 – 153 (2018).
2. A. I. Nizhegorodov, "Technological and energy capabilities of electric two-module pouring furnaces with upper heating system," *Refract. Ind. Ceram.*, **61**(3), 260 – 266 (2020).
3. A. I. Nizhegorodov, A. N. Gavrilin, B. B. Moyses, and G. M. Ismailov, "Modular-pouring furnace with the local granular media flow rates distributed between thermal zones," *Refract. Ind. Ceram.*, **61**(6), 631 – 638 (2020).
4. A. I. Nizhegorodov, *Technologies and Equipment for Vermiculite Processing: Optimal Fractionation, Electric Firing, Re-enrichment*, Izdatel'stvo IrGTU, Irkutsk (2011).
5. V. A. Bauman, I. I. Bykhovsky, *Vibration Machines and Processes in Construction* [in Russian], Vysshaya shkola, Moscow (1977).
6. A. I. Nizhegorodov, "Research of a nonlinear model of a movable hearth platform of an electric furnace for firing loose minerals," *Izvest. Tomsk. Politekhnich. Univ. Inzhinir. Georesurs.*, **330**(9), 172 – 183 (2019).
7. F. Kreith, W. Black, *Fundamentals of Heat Transfer* [translated from English], Mir, Moscow (1983).
8. A. I. Nizhegorodov, Electric Furnace for Obtaining Expanded Vermiculite; Pat. 196953 Russian Federation. IPC F 27 V 9 / 06; applicant and patentee Irkutsk National Research Technical University, Irkutsk, No. 2020100364; submitted 01/13/20; published 03/23/2020, Bul. No. 9.
9. S. S. Kutateladze, *Heat Transfer and Hydrodynamic Resistance: a reference guide* [in Russian], Energoatomizdat, Moscow (1990).
10. N. I. Koshkin, M. G. Shirkevich, *Handbook of Elementary Physics* [in Russian], Izdatel'stvo fiziko-matematicheskoy literatury, Moscow (1972).
11. A. I. Nizhegorodov, "Modeling the transfer of radiant energy to a bulk medium in electric furnaces with the upper position of radiating element," *Refract. Ind. Ceram.*, **61**(1), 25 – 30 (2020).
12. A. V. Zvezdin, T. B. Bryanskikh, and A. I. Nizhegorodov, "Analytical model of absorption-reflection properties of vermiculite under thermal radiation conditions," *Refract. Ind. Ceram.*, **58**(1), 19 – 24 (2017).
13. A. S. Telegin, V. S. Shvydkiy, and Yu. G. Yaroshenko, *Heat and Mass Transfer* [in Russian], ICC "Akadem-kniga", Moscow (2002).
14. A. I. Nizhegorodov, "New factors of reliability of electric furnaces for vermiculite firing with mobile base plates," *Stud Sys. Decis. Control*, **351,** 125 – 138 (2021).